

## **GEOMETRIC ANALYSIS BY CONSTRUCTAL DESIGN OF STIFFENED STEEL PLATES UNDER BENDING WITH TRANSVERSE I-SHAPED OR T-SHAPED STIFFENERS**

**Derick M. P. Kucharski<sup>1</sup>, Vinícius T. Pinto<sup>1</sup>, Luiz A. O. Rocha<sup>1</sup>,  
Elizaldo D. dos Santos<sup>1</sup>, Cristiano Fragassa<sup>2</sup>, Liércio A. Isoldi<sup>1</sup>**

<sup>1</sup>School of Engineering, Federal University of Rio Grande - FURG, Rio Grande, Brazil

<sup>2</sup>Department of Industrial Engineering, University of Bologna, Bologna, Italy

**Abstract.** *Several stiffened plates arrangements subjected to bending were configured applying the Constructal Design Method (CDM) and solved by Finite Element Method (FEM), aiming through the Exhaustive Search (ES) technique analyze the influence of transverse I-Shaped or T-Shaped stiffeners in mechanical behavior. Considering a non-stiffened plate as reference and maintaining the total steel volume constant, a portion of the reference plate was deducted from its thickness, and transformed into stiffeners through the  $\phi$  volume fraction parameter, which represents the ratio between the steel volume of the stiffeners and the steel volume of the reference plate. Assuming  $\phi = 0.3$ , 25 plates with just I-Shaped stiffeners in longitudinal and transverse directions and 25 plates with I-Shaped stiffeners in longitudinal direction and T-Shaped stiffeners in transverse direction were proposed. The results showed that the plates with transverse T-Shaped stiffeners are more effective, reducing the maximum von Mises stress and maximum deflection, respectively, in up to more than 60% and 50% when compared with the plates with just I-Shaped stiffeners.*

**Key words:** *Stiffened plates, Computational modeling, Constructal Design, T-Shaped Stiffeners, I-Shaped Stiffeners*

### 1. INTRODUCTION

Due to the increasingly common engineering trend of building lightweight structures, thin-walled structures have attracted a great deal of attention over the last few decades. Numerous researchers have dedicated their work to provide highly efficient numerical tools to model and simulate the elastic behavior of thin-walled structures [1-4], deal with

---

Received October 16, 2021 / Accepted November 30, 2021

**Corresponding author:** Cristiano Fragassa

Department of Industrial Engineering, University of Bologna, Viale Risorgimento 2, 40136 Bologna, Italy

E-mail: [cristiano.fragassa@unibo.it](mailto:cristiano.fragassa@unibo.it)

their design [5, 6], and buckling issues [7, 8], extend existing methods to isogeometric formulations [9, 10], etc.

Plates are flat, two-dimensional structural components, characterized by their thickness being much smaller than the other two dimensions. One of the most desirable plate features is the great load support resistance with relative low weight, finding application in several engineering areas, such as bridges, aircraft fuselages and ship hulls [11, 12].

Due to the typical high plate slenderness, it is a usual practice to insert reinforcements (stiffeners) in order to increase the flexural rigidity of thin plates. These stiffeners can assume different cross section shapes, being normally welded in the longitudinal and/or transverse directions of the plate [13].

Regarding the structural analysis of non-stiffened thin plates, stresses and displacements can be obtained in a relatively simple way through analytical solutions, applying Navier or Lévy solutions, for instance as well as the Reissner's theory for non-stiffened thick plates [12]. However, when it comes to stiffened plates, analytical solutions are complex and often have limitations related to the boundary conditions and loading, leading to inaccurate results. Hence, numerical solutions became an effective option to solve problems involving stiffened plates. Over the past years, several studies on this topic have been published.

Mukhopadhyay and Satsangi [14] applied the Finite Element Method (FEM) in order to analyze stiffened plates under bending, by means a numerical model employing isoparametric elements, allowing insertion of the transverse shear deformations and curvature limits. Guo et al. [15] focused on the analyses of plates and bridge decks composed by beam-slab system under transverse loading through a semi-discrete finite element formulation, such that the plate-stiffener interaction was considered in terms of bending deflections. Using the Galerkin Method based on First-order Shear Deformable Theory (FSDT). Peng et al. [16] studied the mechanical behavior of stiffened plates subjected to bending, through a meshless approach that allows flexibility in the placement of the stiffeners and expressing the stiffener displacement field as a function of the average surface of the plate.

Taking advantage of the current high-performance computers, commercial software based on numerical methods, mainly the FEM, have been used both in industry and in scientific research. In this sense, a parametric analysis of stiffened plates subjected to bending was carried out by Singh et al. [17] using the ANSYS (FEM commercial software package) considering different loads and boundary conditions. Khosravi et al. [18] analyzed the mechanical behavior of composite steel plate shear walls by means of ABAQUS (FEM commercial software package), Also, Souza et al. [19] showed a topology optimization of stiffened plates using a Modified Adaptive Morphogenesis Algorithm (MAMA), solving different plate arrangements by means of ANSYS.

When it comes to engineering, high structural performance is always a target. Therefore, regarding steel plates, the Constructal Design Method (CDM) associated with computational modeling by FEM, have reached interesting results, as in: Isoldi et al. [20, 21], Helbig et al. [22-24], Da Silva et al. [25], and Da Silveira et al. [26] who investigated the buckling effect on perforated plates; Lima et al. [27, 28] who analyzed the buckling of stiffened plates; and Cunha et al. [29, 30], De Queiroz et al. [31], Troina et al. [32], Nogueira et al. [33], and Pinto et al. [34, 35] who studied the bending of plates with I-Shaped stiffeners.

Given the above, this work focused on the geometric evaluation and optimization of stiffened plates subjected to bending concerning the influence of the stiffeners cross section geometry, with I-Shaped stiffeners in the longitudinal direction and I-Shaped or T-Shaped stiffeners in the transverse direction. To do so, several stiffened plates arrangements were

defined using CDM, solved by FEM, and compared among each other through the Exhaustive Search (ES) technique, allowing identifying the transverse stiffener geometry influence on the maximum von Mises stress and maximum deflection, as well as to indicate the optimized configuration that minimizes these performance indicators.

## 2. METHODOLOGY

### 2.1. Computational Modeling

In this study, all computational models were solved by FEM using the ANSYS software, considering a linear-elastic material behavior and a geometric linear structural analysis. The discretization of the computational domains was performed applying the two-dimensional finite element SHELL281 in its quadrilateral version. This finite element is suitable for modeling thin and moderately thick plates, has 8 nodes with 6 degrees of freedom per node: 3 translations and 3 rotations related to  $x$ ,  $y$  and  $z$  axes; being based on the first-order shear-deformation theory (or Mindlin-Reissner shell theory) [36].

#### 2.1.1. Computational Model Verification

The computational model verification was carried out based on the stiffened plate presented at Fig. 1, which was previously solved by Troina et al. [37] using a regular mesh composed of 3,928 three-dimensional finite element SOLID95 in its hexahedral version by ANSYS.

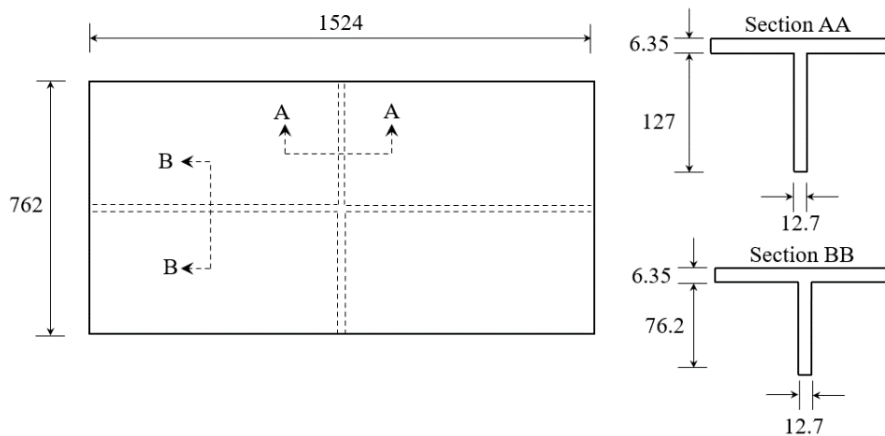


**Fig. 1** Stiffened plate used in the numerical model verification (unit: mm)

The simply supported stiffened steel plate of Fig. 1 has elastic modulus of 206.8427 GPa and Poisson's ratio of 0.3, being subjected to a uniform normal loading of 68.95 kPa. The case was solved using 15,200 SHELL281 finite elements in its quadrilateral version, defined from the convergence test presented in Fig. 2. Figure 2 also shows the result obtained by Troina et al. [37] for the central deflection of the stiffened plate.

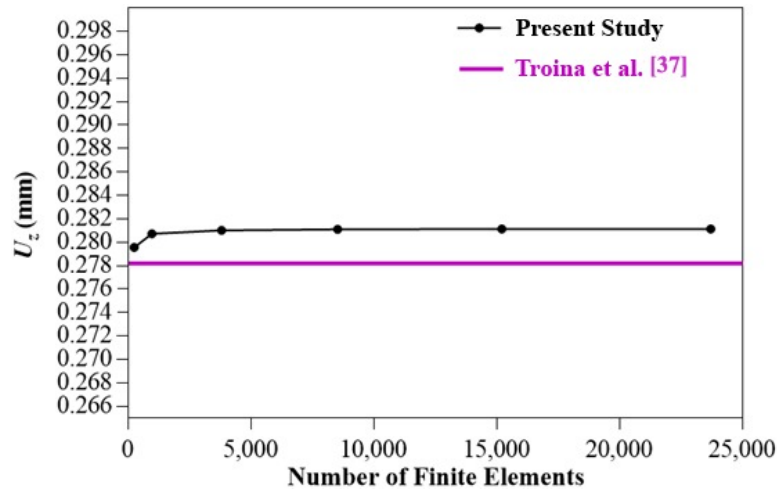


**Fig. 2** Mesh convergence test and computational model verification

From Fig. 2, it is perceptible that the difference concerning the central deflection  $U_z$  is about 1%, comparing the present study using the 2-D finite element SHELL281 and the result presented by Troina et al. [37] with the 3-D finite element SOLID95, verifying the computational model.

### 2.1.2. Computational Model Validation

The experimental case adopted to validate the computational modeling was presented by Carrijo et al. [38], as shown in Fig. 3. The acrylic stiffened plate was subjected to a uniform normal load of 0.96 kPa, having an elastic modulus of 2.5 GPa and a Poisson's ratio of 0.36. With respect to the boundary conditions, just its four corners were considered simply supported.

In the present study the case of Fig. 3 was numerically reproduced using the SHELL281 quadrilateral finite element with a mesh of 2,436 computational cells, established according to the mesh convergence test presented in Fig. 4, which also shows the result experimentally obtained by Carrijo et al. [38].

By analyzing the Fig. 4, it is possible to notice that the numerical result for the central deflection of the plate  $U_z = 6.505$  mm, represents a difference of 4.58% when compared with the value of  $U_z = 6.220$  mm obtained in the experimental study, validating the computational model.

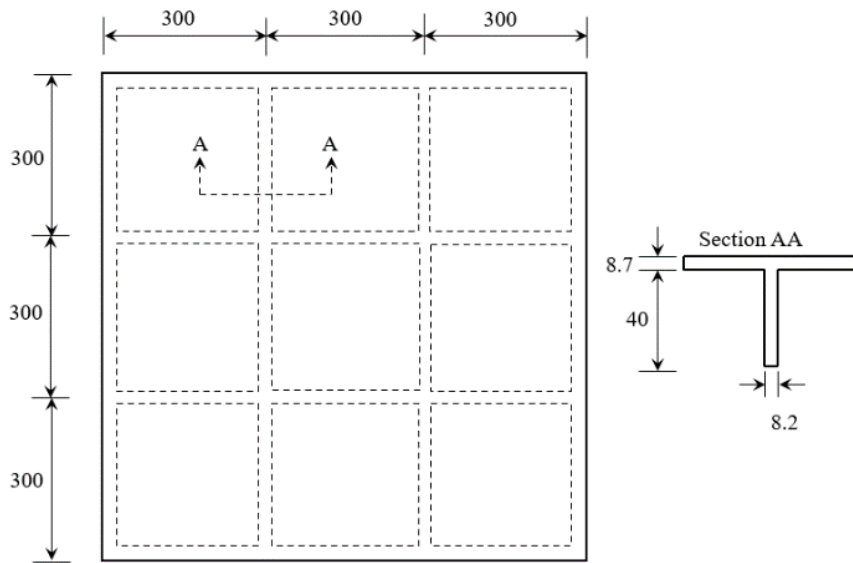


**Fig. 3** Stiffened plate used in the numerical model validation (unit: mm)

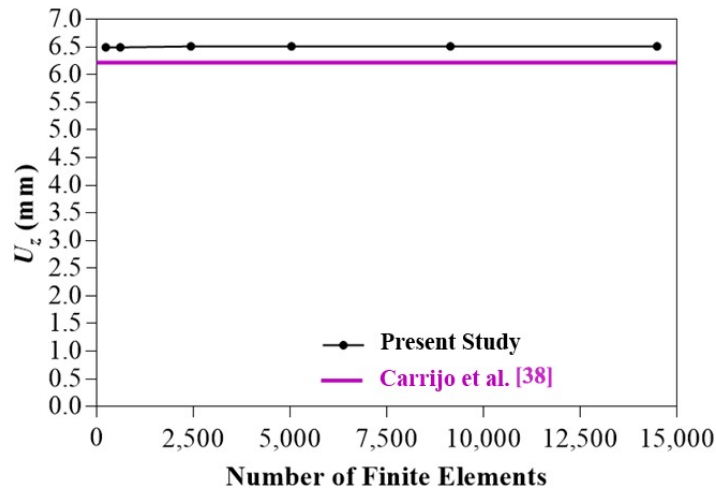


**Fig. 4** Mesh convergence test and computational model validation

## 2.2. Constructal Design Method (CDM)

The Constructal Theory brings the comprehension that the design of all flow systems (such as the atmospheric electrical discharges, deltas of rivers, roots and branches of trees, veins and arteries of the human body, social dynamics, engineering and technology and so on) are generated by a physical phenomenon named as Constructal Law [39]. The Constructal Law states: "For a finite-size flow system to persist in time (to live), its configuration must evolve in such a way that provides greater and greater access to the

currents that flow through it" [40]. According to Rocha et al. [41], the Constructal Law is about the evolution direction in time, i.e., the design phenomenon is a dynamic and continuous process.

The Constructal Law is applied in engineering flow systems by means the Constructal Design Method (CDM). The CDM is a geometric evaluation method and its application demands the definition of constraints (global or local), degrees of freedom (free to vary, respecting the constraints) and performance indicators that can be maximized or minimized (which represents a view of ease of flow access). However, if the goal is to define the optimized geometric configuration, the CDM must be employed in association with an optimization method (such as Exhaustive Search or Heuristic Methods). In this case, the CDM is responsible for creating the search space (containing the possible geometric configurations) while the optimization method is in charge of identify the system geometry that leads to the superior performance [26, 41, 42].

In this work, the CDM application started from a non-stiffened steel plate taken as reference, with length  $a = 2000$  mm, width  $b = 1000$  mm and thickness  $t = 20$  mm. Thereafter, maintaining constant the total material volume and the dimensions  $a$  and  $b$ , a portion of material fully deducted from the thickness of the reference plate was transformed into stiffeners through a parameter named volume fraction  $\phi$  (ratio between the steel volume of stiffeners and the steel volume of the reference plate). According to Troina et al. [32], the value of  $\phi$  adopted in this study was 0.3, which means that 30% of the non-stiffened plate volume (reference plate) was converted into stiffeners. Due to this, the thickness of the stiffened plate became  $t_p = 14$  mm.

A total of 50 stiffened plates' arrangements were analyzed: 25 with only I-Shaped stiffeners in both directions and 25 with I-Shaped stiffeners in longitudinal direction and T-Shaped stiffeners in transverse direction, with the main purpose to analyze the stiffeners influence over the maximum out-of-plane displacement (deflection) and the maximum von Mises stress. It is important to highlight that the choice to study the transverse stiffeners cross section shape influence is based on Nogueira et al. [33], where it was inferred that the transverse stiffeners are more effective for the reduction of the maximum and central deflections of stiffened plates.

The mathematical definition of the volume fraction  $\phi$  for plates with just I-Shaped in both directions and having I-Shaped stiffeners in longitudinal direction and T-Shaped in transverse direction are, respectively, given by:

$$\phi = \frac{V_s}{V_r} = \frac{n_{sx}(ah_s t_s) + n_{sy}[(b - n_{sx}t_s)h_s t_s]}{abt} \quad (1)$$

$$\phi = \frac{V_s}{V_r} = \frac{[n_{sx}(ah_s t_s) + n_{sy}(bh_w t_w + ba_f t_f)] - V_{in}}{abt} \quad (2)$$

where  $V_s$  is the material volume of the stiffeners and  $V_r$  is the material volume of the reference plate. The height and thickness of the I-Shaped stiffeners are  $h_s$  (variable) and  $t_s$  (kept constant and equal to 8 mm). Concerning the T-Shaped stiffeners,  $t_w$  and  $t_f$  represent the thickness of the web and flange, respectively, both considered with 8 mm. The height of the web is named  $h_w$  (variable), the length of the flange is  $a_f$  (considered as half of the web height, i.e.,  $a_f = 0.5h_w$ ), and the stiffeners intersection volume is  $V_{in}$ . Moreover, the number of stiffeners in  $x$  (longitudinal) and  $y$  (transverse) directions are, respectively,  $n_{sx}$  and  $n_{sy}$ , being ranged from 2 to 6.

In addition, to identify the stiffened plate arrangements, the following nomenclature was adopted:  $P_I(n_{sx}, n_{sy})$  to the I-Shaped stiffened plates and  $P_T(n_{sx}, n_{sy})$  to the T-Shaped and I-Shaped stiffened plates. All of these aforementioned parameters can be seen at Figs. 5 and 6; while Fig. 7(a) shows the search space defined by the CDM application and Fig. 7(b) presents a step by step of the methodology adopted in this work.

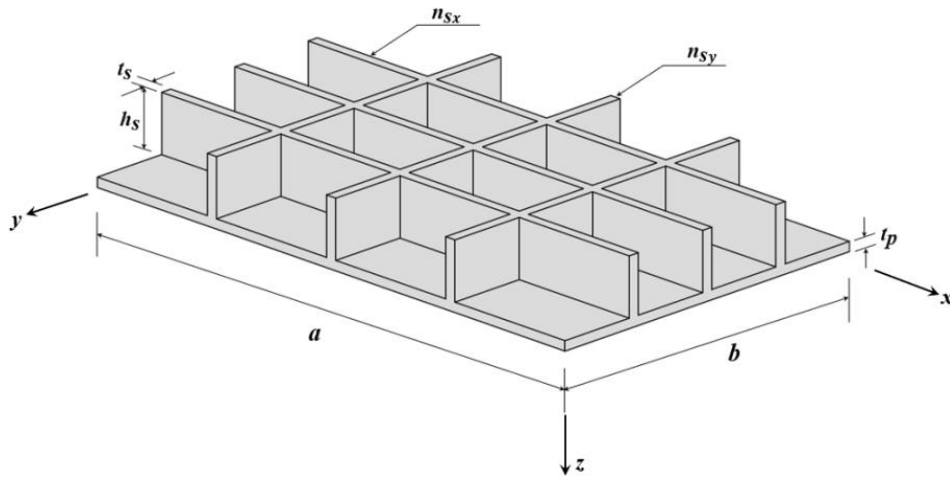


**Fig. 5** Geometric parameters of stiffened plate  $P_I(3,3)$

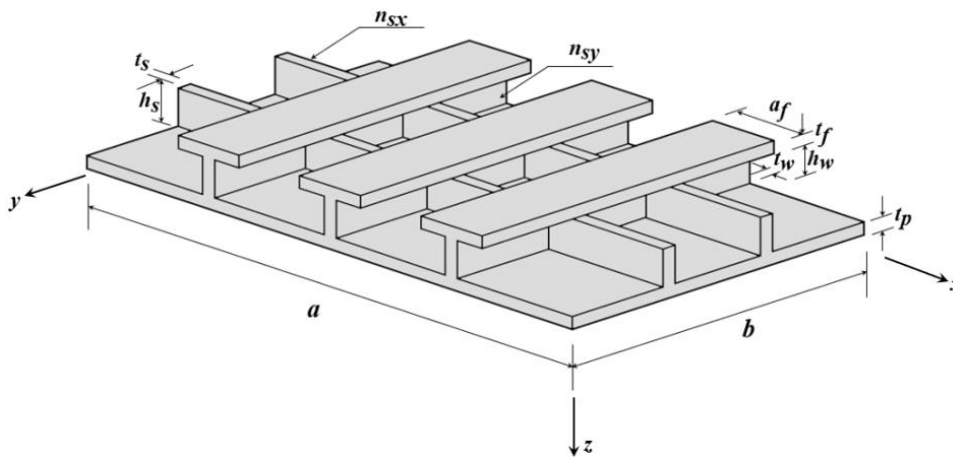


**Fig. 6** Geometric parameters of stiffened plate  $P_T(2,3)$

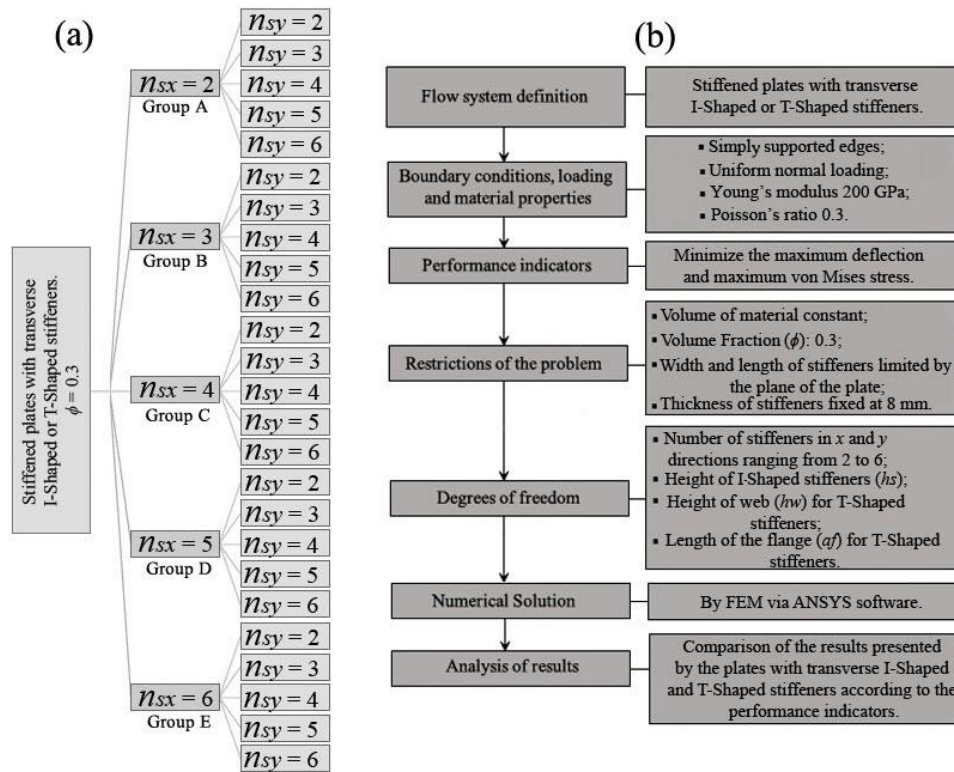


**Fig. 7** (a) Search space defined by CDM; (b) Methodology of the study

It is important to mention that all geometric configurations of the search space (see Fig. 7(a)) were numerically simulated and the results compared to each other, thus performing an optimization procedure by means of an Exhaustive Search (ES) technique.

### 3. RESULTS AND DISCUSSION

As in De Queiroz et al. [31] and Troina et al. [32], all stiffened plates analyzed in this study (see Fig. 7(a)) were considered with boundary conditions of simply supported edges and subjected to a uniform normal loading of 10 kPa. Regarding the material, it was adopted the A-36 steel with Poisson's ratio 0.30, Young's modulus 200 GPa, and yield strength of 250 MPa.

In order to define the suitable size of finite elements used to discretize all computational models, a mesh convergence test was performed considering the more complex geometry  $P_1(6,6)$  among all proposed stiffened plates, concerning the maximum von Mises stress. According Troina et al. [32], several meshes were considered taking as reference the plate width  $b$ . The result of the mesh convergence test can be observed in Fig. 8(a) and the successive mesh refinements are indicated in Fig. 8(b).



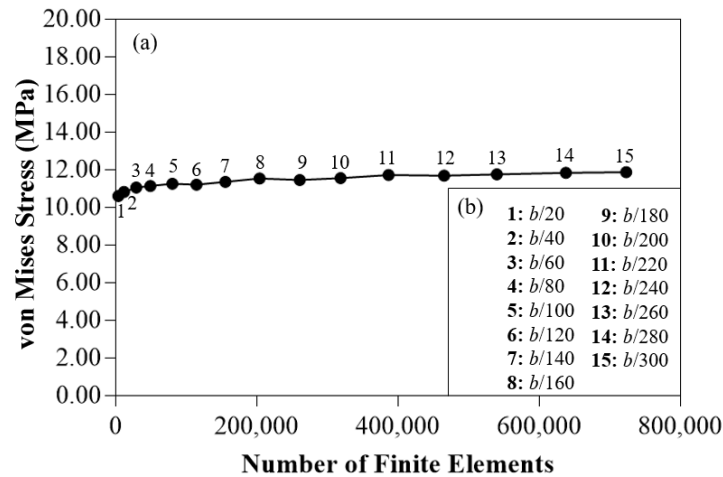


**Fig. 8** Mesh convergence test: (a) maximum von Mises stress variation; (b) mesh refinement criteria

Observing the results of Fig. 8(a), it can be noted that from the mesh number 11, there was a stabilization trend for the stress value. Therefore, the refinement  $b/220$  with a finite element size of 4.55 mm was adopted to discretize all computational domains investigated in this study. The results of the stiffened plates, for maximum von Mises stress and maximum deflection are presented in Figs. 9 and 10, respectively. The bar graph format was chosen to allow a direct observation between variations of stresses and deflections occurred in the plates with only I-Shaped stiffeners and with T- and I-Shaped stiffeners.

A first finding emerging from Figs. 9 and 10 is that the conversion of a portion of material from the non-stiffened reference plate, keeping the total material volume constant, according to the main CDM premise, causes an increase in the plate stiffness, once all values of maximum deflection are lower than the value reached by the reference plate of  $U_z = 0.697$  mm. When it comes to the maximum von Mises stress, most of the stiffened plates with just I-Shaped stiffeners presented values greater than the value of 13.313 MPa obtained by the non-stiffened reference plate. Meantime, concerning the plates with transverse T-Shaped and longitudinal I-Shaped stiffeners, in all cases, the maximum von Mises stress value is lower than 13.313 MPa of the reference plate.

It is well known that in structural engineering focused on design of flat components, whether in metallic (present study) or reinforced concrete (e.g., slabs) structures, deflection and stress are important parameters. The deflection is a serviceability parameter which not necessarily compromise the safety, as long as, the values presented are in accordance with design standards. On the other hand, values of stress are directly related with safety, i.e., if exceeded the maximum limits the structure is on the verge of collapse [43]. Therefore, in this study it was chosen as main parameter the maximum von Mises stress following by the maximum deflection, i.e., the criterion that qualify the better stiffened plate arrangement in each group of plates (see Fig.7(a)) is the maximum von Mises stress.

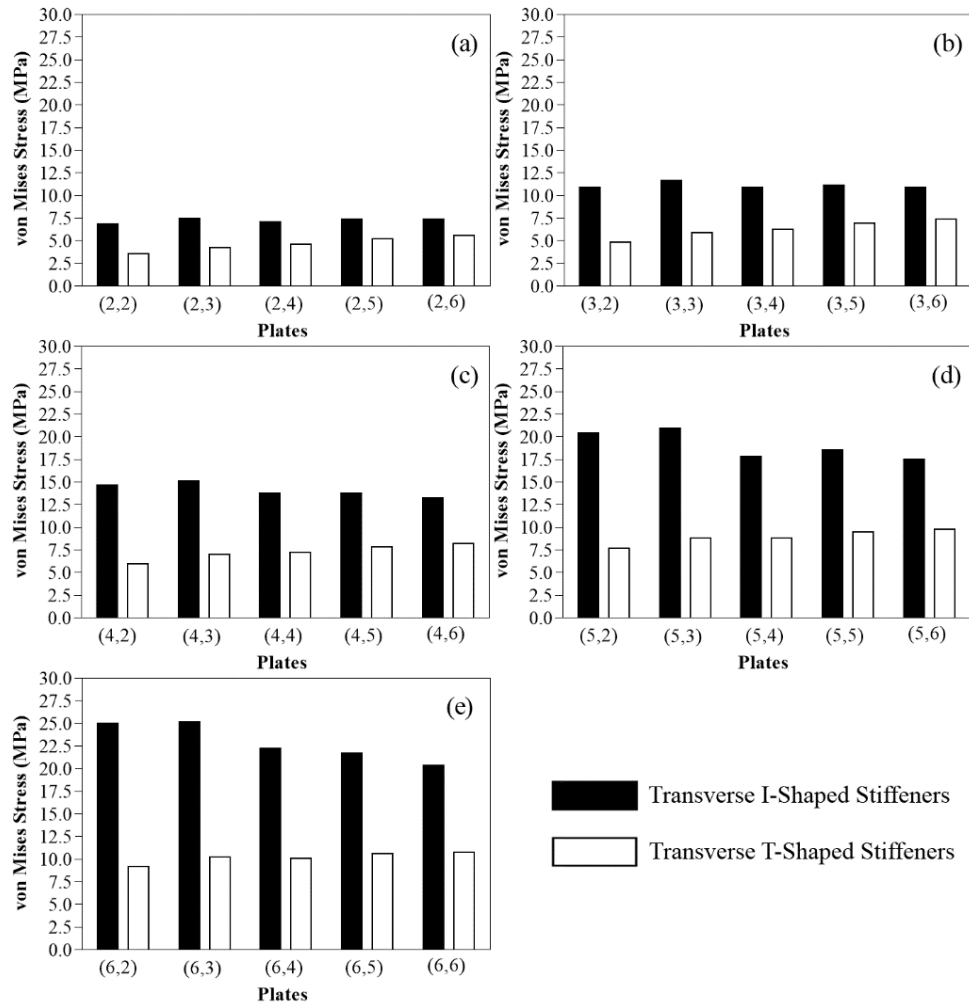


**Fig. 9** Results of maximum von Mises stress: (a) Group A; (b) Group B; (c) Group C; (d) Group D; (e) Group E

That said, Figs. 9(a) and 10(a) (Group A) indicate that the plate with better mechanical behavior was  $P_T(2,2)$ , having a maximum von Mises stress of 3.581 MPa, which represents a minimization of 48.2% in comparison with the value of 6.920 MPa of the plate  $P_I(2,2)$ . Concerning the maximum deflection, the plate  $P_T(2,2)$  presents 0.023 mm, representing a slight reduction of 8.7% if compared with the plate  $P_I(2,2)$  that achieved  $U_z = 0.025$  mm.

In turn, with respect to the Group B (see Figs. 9(b) and 10(b)) the plate  $P_T(3,2)$  showed superior performance among all arrangements. Comparing the von Mises stress value of 4.825 MPa obtained by the plate  $P_T(3,2)$  with the value of 10.957 MPa found for the plate  $P_I(3,2)$ , it is reached a reduction of 55.96%. Still on Group B, regarding the maximum deflection the plate  $P_T(3,2)$  achieved a minimization of 29.4% in comparison with the plate  $P_I(3,2)$ , being the maximum deflection values of 0.026 mm and 0.037 mm, respectively.

For the Group C, as showed at Figs. 9(c) and 10(c), one can note that the plates containing T- and I-Shaped stiffeners tend to present a better performance than the plates with only I-Shaped stiffeners for both performance parameters. The best performance was obtained by the plate  $P_T(4,2)$ , reducing the maximum von Mises stress (of 5.976 MPa) and maximum deflection (of 0.035 mm) in 59.3% and 41.2%, respectively, in comparison with the plate  $P_I(4,2)$  that showed von Mises stress equal to 14.678 MPa and maximum deflection of 0.059 mm.

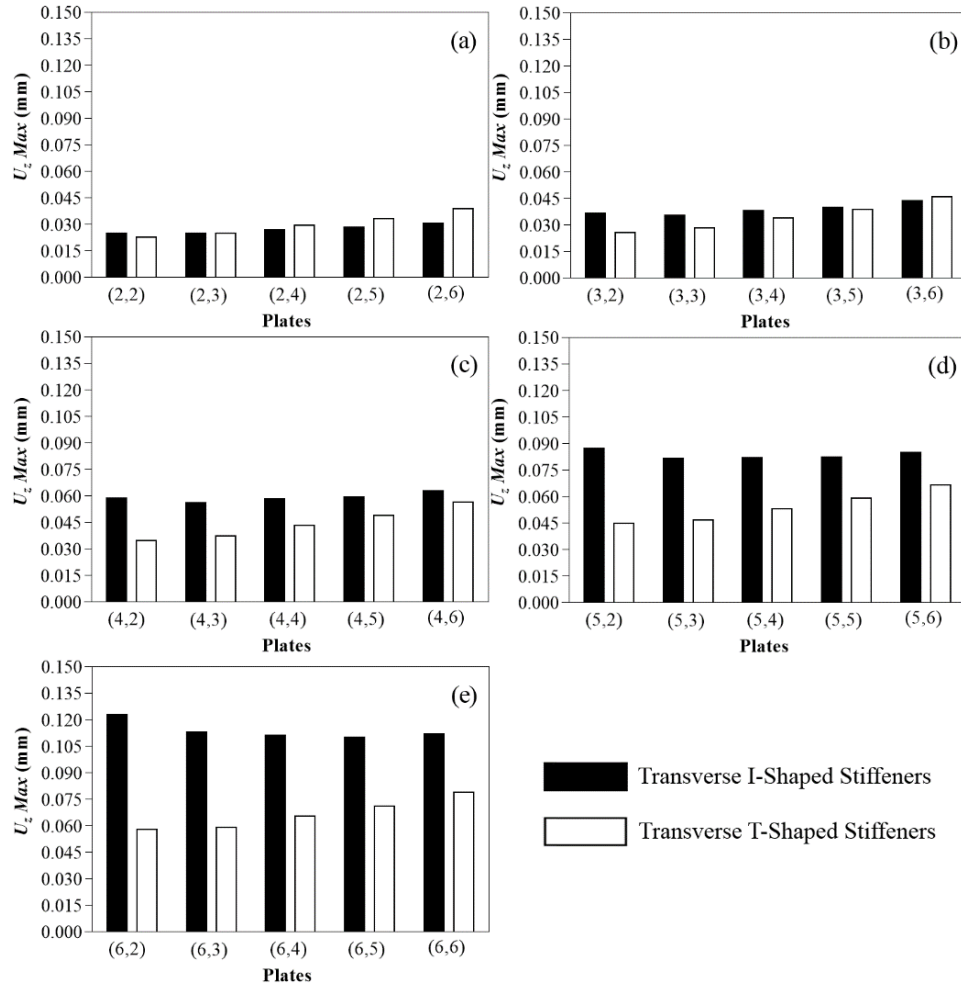


**Fig. 10** Results of maximum deflection: (a) Group A; (b) Group B; (c) Group C; (d) Group D; (e) Group E

In sequence, analyzing the results of Group D in Figs. 9(d) and 10(d), the plate  $P_T(5,2)$  achieved the best mechanical behavior with a von Mises stress of 7.716 MPa and a maximum deflection of 0.045 mm. If  $P_T(5,2)$  is compared with  $P_I(5,2)$ , that reached

maximum values of 20.488 MPa and 0.087 mm, reductions of 62.3% for maximum von Mises stress and 48.6% for maximum deflection were observed.

Lastly, when it comes to the Group E (see Figs. 9(e) and 10(e)), the superior performance was presented by the plate  $P_T(6,2)$ , with maximum von Mises stress of 9.231 MPa and maximum deflection of 0.058 mm; meaning a decrease in comparison with the plate  $P_I(6,2)$  of 63.0% for the von Mises stress (of 25.0 MPa) and 52.9% for maximum deflection (of 0.123 mm).

Among all analyzed groups, the Group E achieved the highest percentage reductions in the performance indicators. For this reason, aiming to illustrate these mechanical behaviors, Figs. 11 and 12 depicted, respectively, the stress and deflection distributions for the stiffened plates  $P_T(6,2)$  and  $P_I(6,2)$ .

From Fig. 11, one can note that the maximum von Mises stress of 25.0 MPa occurs in the transverse I-Shaped stiffeners region farthest from the plate (Fig. 11(b)). In addition, keeping constant the total amount of material and just changing the geometric configuration of the cross section of the transverse stiffeners from I-Shaped to T-Shaped, the flow of stress is better distributed and a significantly lower von Mises stress magnitude is reached (Fig. 11(a)).

Likewise, in Fig. 12, it is possible to observe the influence of the geometric configuration in the out-of-plane displacements distributions provided by the CDM application, allowing reducing the maximum deflection by more than 50% when using the T-Shaped instead of the I-Shaped in transverse stiffeners.

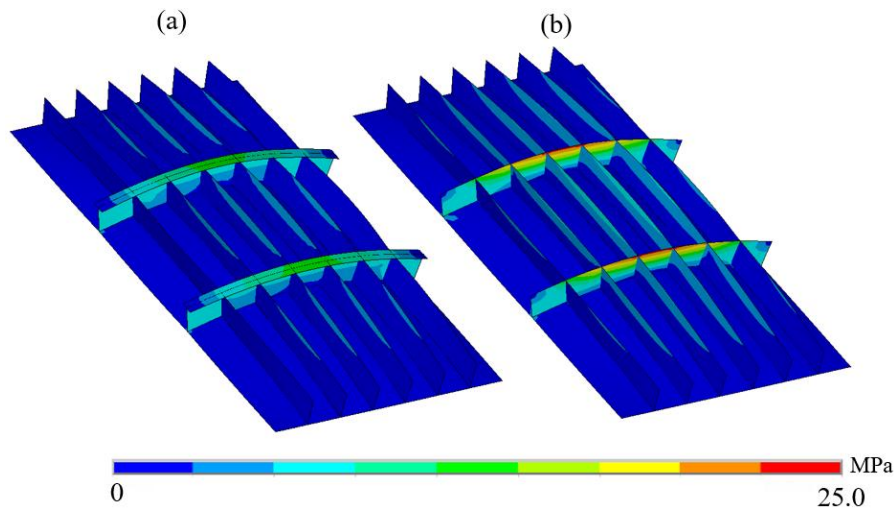


**Fig. 11** Distribution of the von Mises stresses: (a)  $P_T(6,2)$ ; (b)  $P_I(6,2)$

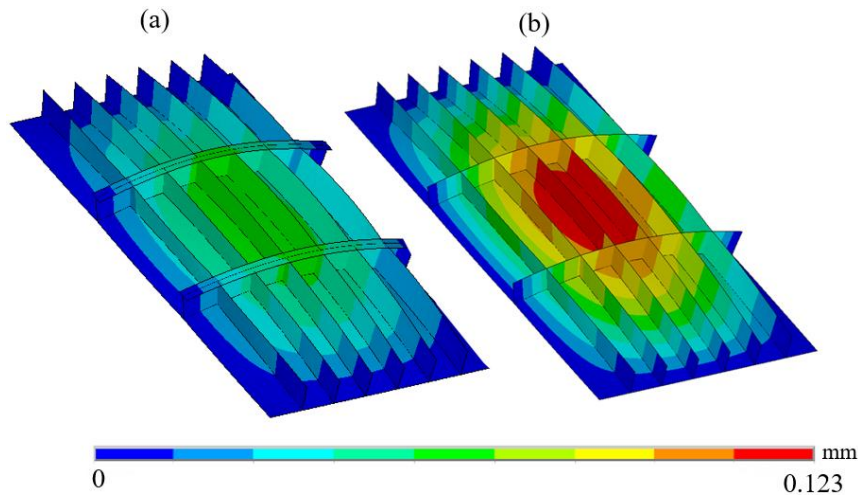


**Fig. 12** Distribution of the deflections: (a)  $P_T(6,2)$ ; (b)  $P_I(6,2)$

It is important to emphasize that the superior performance of the plates with transverse T-Shaped stiffeners when compared with the plates with transverse I-Shaped stiffeners (see Figs. 9 and 10) can be explained through the influence of the moment of inertia of the stiffeners cross section. The moment of inertia of the T-Shaped stiffeners is greater than the moment of inertia of the I-Shaped stiffeners, considering the same amount of material according to CDM. To exemplify, the Table 1 shows the moments of inertia per stiffener for the aforementioned plates that presents best performance in each group (see Figs. 7(a), 9, and 10).

**Table 1** Transverse stiffener’s moment of inertia for the plates with the better performance

Plates	Moment of Inertia ( $10^6 \text{ mm}^4$ )	
	I-Shaped Stiffener	T-Shaped Stiffener
(2,2)	10.585	13.809
(3,2)	4.474	6.582
(4,2)	2.293	3.650
(5,2)	1.328	2.237
(6,2)	0.837	1.473

It is worth to mention that the comparison presented in Table 1 serves only to illustrate the difference of the moment of inertia of the stiffeners cross section in a simple way, justifying its direct influence in the overall behavior of the stiffened plates.

#### 4. CONCLUSION

Several rectangular plates arrangements with I-Shaped stiffeners in longitudinal direction and with I-Shaped or T-Shaped stiffeners in transverse direction were evaluated regarding to the maximum von Mises stress and the maximum deflection applying CDM, FEM and ES technique.

Initially it was inferred that converting a material portion of a non-stiffened steel plate (deducted entirely of its thickness) into stiffeners, while maintaining the total material volume, is effective to significantly reduce the maximum deflection of the plate. However, concerning the maximum von Mises stress, the plates with transverse I-Shaped stiffeners can reach values higher than the one reached by the reference plate; while all the plates having transverse T-Shaped stiffeners achieved inferior magnitudes for the maximum von Mises stress if compared with reference plate.

It was also concluded that for the vast majority of stiffened plates analyzed, those with transverse T-Shaped stiffeners presented better performance than the plates with only I-Shaped stiffeners, being able to minimize up to more than 60% the maximum von Mises stress and up to more than 50% the maximum deflection, such as plates  $P_{T(6,2)}$  and  $P_{I(6,2)}$ .

These aspects show the relevance of geometric evaluation in structural engineering, since the amount of material of the plates was kept constant and the mechanical behavior was considerably improved only due to the change in the geometric configuration of the stiffeners.

Therefore, based on the positive results achieved here, as well as in the previous studies, it would be interesting to apply the presented approach in future works in order to investigate other values of volume fraction  $\phi$ , different aspect ratios  $a/b$  for the plate, and another shapes of stiffeners. One may expect that a similar trend of improvement would be achieved.

**Acknowledgement:** *This work was performed with the support of the: Coordenação de Aperfeiçoamento de Pessoal de Nível Superior – Brazil (CAPES) – Finance Code 001, Fundação de Amparo à Pesquisa do Estado do Rio Grande do Sul – Brazil (FAPERGS) and Conselho Nacional de Desenvolvimento Científico e Tecnológico – Brazil (CNPq). Particularly, the authors L.A.O. Rocha, E.D. dos Santos and L.A. Isoldi thank to CNPq for their research grants (Processes: 307791/2019-0, 306024/2017-9 and 306012/2017-0, respectively).*

## REFERENCES

1. Rama, G., Marinkovic, D., Zehn, M., 2018, *High performance 3-node shell element for linear and geometrically nonlinear analysis of composite laminates*, Composites Part B: Engineering, 151, pp. 118-126.
2. Marinković, D., Rama, G., Zehn, M., 2019, *Abaqus implementation of a corotational piezoelectric 3-node shell element with drilling degree of freedom*, Facta Universitatis-Series Mechanical Engineering, 17(2), pp. 269-283.
3. Pagani, A., Azzara, R., Augello, R., Carrera, E., *Stress states in highly flexible thin-walled composite structures by unified shell model*, AIAA Journal, doi: 10.2514/1.J060024.
4. Marinković, D., Marinković, Z., 2012, *On FEM modeling of piezoelectric actuators and sensors for thin-walled structures*, Smart Structures and Systems, 9(5), pp. 411-426.
5. Liu, Z., Niu, J., Jia, R., Guo, J., 2021, *An efficient numerical method for dynamic analysis of polygonal plate under moving loads*, Thin-Walled Structures, 167, 108183.
6. Khaloo, A., Ghamari, A., Foroutani, M., 2021, *On the design of stiffened steel plate shear wall with diagonal stiffeners considering the crack effect*, Thin-Walled Structure, 31, pp. 828-841.
7. Kövesdi, B., Haffar, M.Z., Ádany, S., 2021, *Buckling resistance of longitudinally stiffened plates: Eurocode-based design for column-like and interactive behavior of plates with closed-section stiffeners*, Thin-Walled Structures, 159, 107266.
8. Feng, L., Sun, T., Ou, J., 2021, *Elastic buckling analysis of steel-strip-stiffened trapezoidal corrugated steel plate shear walls*, Journal of Constructional Steel Research, 184, 106833.
9. Benson, D.J., Bazilevs, Y., Hsu, M.C., Hughes, T.J.R., 2010, *Isogeometric shell analysis: The Reissner-Mindlin shell*, Computer Methods in Applied Mechanics and Engineering, 199(5-8), pp. 276-289.
10. Milić, P., Marinković, D., 2015, *Isogeometric FE analysis of complex thin-walled structures*, Transactions of Famena, 39(1), pp. 15-26.

11. Ventsel, E., Krauthammer, T., 2001, *Thin Plates and Shells: Theory, Analysis and Applications*, CRC Press.
12. Szilard, R., 2004, *Theories and Applications of Plate Analysis: Classical, Numerical and Engineering Methods*, John Wiley & Sons, Inc.
13. Bedair, O.K., 2009, *Analysis and limit state design of stiffened plates and shells: a world view*, Applied Mechanics Reviews, 62(2), 020801.
14. Mukhopadhyay, M., Satsangi, S.K., 1984, *Isoparametric stiffened plate bending element for the analysis of ship's structure*, Royal Institution of Naval Architects Transactions, 126, pp. 141-151.
15. Guo, M., Issam, E.H., Ren, W., 2002, *Semi-discrete finite element analysis of slab-girder bridges*, Computers & Structures, 80(23), pp. 1789-1796.
16. Peng, L.X., Kitipornchai, S., Liew, K.M., 2005, *Analysis of rectangular stiffened plates under uniform lateral load based on FSDT and element-free Galerkin method*, International Journal of Mechanical Sciences, 47(2), pp. 251-276.
17. Singh, D.K., Duggal, S.K., Pal, P., 2015, *Analysis of stiffened plates using FEM - a parametric study*, International Research Journal of Engineering and Technology, 2(4), pp. 1650-1656.
18. Khosravi, H., Mousavi, S.S., Tadayonfar, G., 2017, *Numerical study of seismic behavior of composite steel plate shear walls with flat and corrugated plates*. Revista de la Construcción, 16(2), pp. 249-260.
19. Souza, B.F., Anflor, C.T.M., Jorge, A.B., 2021, *Application of modified adaptive morphogenesis and robust optimization algorithms for thin stiffened plates*, Engineering with Computers, doi: 10.1007/s00366-021-01465-w.
20. Isoldi, L.A., Real, M.V., Correia, A.L.G., Vaz, J., Dos Santos, E.D., Rocha, L.A.O., 2013, *Flow of Stresses: Constructal Design of Perforated Plates Subjected to Tension or Buckling*, In: Rocha, L.A.O., Lorente, S., Bejan, A. (Ed.), *Constructal Law and the Unifying Principle of Design - Understanding Complex Systems*, Springer.
21. Isoldi, L.A., Real, M.V., Vaz, J., Correia, A.L.G., Dos Santos, E.D., Rocha, L.A.O., 2013, *Numerical analysis and geometric optimization of perforated thin plates subjected to tension or buckling*, Marine Systems & Ocean Technology, 8(2), pp. 99-107.
22. Helbig, D., Da Silva, C.C.C., Real, M.V., Dos Santos, E.D., Isoldi, L.A., Rocha, L.A.O., 2016, *Study about buckling phenomenon in perforated thin steel plates employing computational modeling and Constructal Design method*, Latin American Journal of Solids and Structures, 13, pp. 1912-1936.
23. Helbig, D., Real, M.V., Dos Santos, E.D., Isoldi, L.A., Rocha, L.A.O., 2016, *Computational modeling and Constructal Design method applied to the mechanical behavior improvement of thin perforated steel plates subject to buckling*. Journal of Engineering Thermophysics, 25, pp. 197-215.
24. Helbig, D., Cunha, M.L., Da Silva, C.C.C., Dos Santos, E.D., Iturrioz, I., Real, M.V., Isoldi, L.A., Rocha, L.A.O., 2018, *Numerical study of the elasto-plastic buckling in perforated thin steel plates using the Constructal Design method*. Research on Engineering Structures and Materials, 4(3), pp. 169-187.
25. Da Silva, C.C.C., Helbig, D., Cunha, M.L., Dos Santos, E.D., Rocha, L.A.O., Real, M.V., Isoldi, L.A., 2019, *Numerical buckling analysis of thin steel plates with centered hexagonal perforation through Constructal Design method*, Journal of the Brazilian Society of Mechanical Sciences and Engineering, 41(8), 309.
26. Da Silveira, T., Pinto, V.T., Neufeld, P.D.S., Pavlovic, A., Rocha, L.A.O., Dos Santos, E.D., Isoldi, L. A., 2021, *Applicability evidence of Constructal Design in structural engineering: case study of biaxial elasto-plastic buckling of square steel plates with elliptical cutout*, Journal of Applied and Computational Mechanics, 7(2), pp. 922-934.
27. Lima, J.P.S., Rocha, L.A.O., Dos Santos, E.D., Real, M.V., Isoldi, L.A., 2018, *Constructal Design and numerical modeling applied to stiffened steel plates submitted to elasto-plastic buckling*, Proceedings of the Romanian Academy Series A-Mathematics Physics Technical Sciences Information Science, 19, pp. 195-200.
28. Lima, J.P.S., Cunha, M.L., Dos Santos, E.D., Rocha, L.A.O., Real, M.V., Isoldi, L.A., 2020, *Constructal Design for the ultimate buckling stress improvement of stiffened plates submitted to uniaxial compressive load*, Engineering Structures, 203, 109883.
29. Cunha, M.L., Troina, G.S., Rocha, L.A.O., Dos Santos, E.D., Isoldi, L.A., 2018, *Computational modeling and Constructal Design method applied to the geometric optimization of stiffened steel plates subjected to uniform transverse load*, Research on Engineering Structures and Materials, 4(3), pp. 139-149.
30. Cunha, M.L., Estrada, E.S.D., Lima, J.P.S., Troina, G.S., Dos Santos, E.D., Isoldi, L.A., 2020, *Constructal design associated with genetic algorithm to minimize the maximum deflection of thin stiffened steel plates*, Heat Transfer, 49(7), pp. 4040-4055.
31. De Queiroz, J.P.T.P., Cunha, M.L., Pavlovic, A., Rocha, L.A.O., Dos Santos, E.D., Troina, G.S., Isoldi, L.A., 2019, *Geometric evaluation of stiffened steel plates subjected to transverse loading for naval and offshore applications*, Journal of Marine Science and Engineering, 7(1), pp. 7-18.

32. Troina, G.S., Cunha, M.L., Pinto, V.T., Rocha, L.A.O., Dos Santos, E.D., Fragassa, C., Isoldi, L.A., 2020, *Computational modeling and Design Constructal theory applied to the geometric optimization of thin steel plates with stiffeners subjected to uniform transverse load*, *Metals*, 10(2), 220.
33. Nogueira, C.M., Pinto, T.V., Rocha, L.A.O., Dos Santos, E.D., Isoldi, L.A., 2021, *Numerical simulation and Constructal Design applied to plates with different heights of traverse and longitudinal stiffeners*, *Engineering Solid Mechanics*, 9(2), pp. 221-238.
34. Pinto, V.T., Rocha, L.A.O., Fragassa, C., Dos Santos, E.D., Isoldi, L.A., 2020, *Multiobjective geometric analysis of stiffened plates under bending through Constructal Design method*, *Journal of Applied and Computational Mechanics*, 6, pp. 1438-1449.
35. Pinto, V.T., Cunha, M.L., Martins, K.L., Rocha, L.A.O., Dos Santos, E.D., Isoldi, L.A., 2021, *Bending of stiffened plates considering different stiffeners orientations*, *Magazine of Civil Engineering*, 103(3), 10310.
36. ANSYS, 2011, *ANSYS Mechanical APDL Element Reference - Release 14.0*, ANSYS, Inc.
37. Troina, G.S., De Queiroz, J.P.T.P., Cunha, M.L., Rocha, L.A.O., Dos Santos E.D., Isoldi, L.A., 2018, *Verificação de modelos computacionais para placas com enrijecedores submetidas a carregamento transversal uniforme*, *CEREUS*, 10(2), pp. 285-298, (in Portuguese).
38. Carrijo, E.C., Paiva, J.B., Giogo, J.S., 1999, *A numerical and experimental study of stiffened plates in bending*, *Transactions on Modelling and Simulation*, 21, pp. 12-18.
39. Bejan, A., Zane, J.P., 2012, *Design in Nature: How the Constructal Law Governs Evolution in Biology, Physics, Technology, and Social Organizations*, Doubleday.
40. Bejan, A., Lorente, S., 2008, *Design with Constructal Theory*, John Wiley & Sons, Inc.
41. Rocha, L.A.O., Lorente, S., Bejan, A., 2018, *Constructal Theory in Heat Transfer*, In: Kulacki, F. (Ed.), *Handbook of Thermal Science and Engineering*, Springer.
42. Dos Santos, E.D., Isoldi, L.A., Gomes, M.N., Rocha, L.A.O., 2017, *The Constructal Design Applied to Renewable Energy Systems*, In: Rincón-Mejía, E., De las Heras, A. (Eds.), *Sustainable Energy Technologies*, CRC Press.
43. Salmon, C.G., Johnson, J.R., Malhas, F.A., 2009, *Steel Structures: Design and Behavior*, Pearson.